Biochemical Engineering Journal 213 (2025) 109552

Contents lists available at ScienceDirect

Biochemical Engineering Journal

journal homepage: www.elsevier.com/locate/bej

Regular article

Development of inducible packaging cell line for rAAV production via CRISPR-Cas9 mediated site-specific integration

Qiang Fu [a], Yongdan Wang [b], Emily Doleh [c], Mark Blenner [c], Seongkyu Yoon [a,b,*]

[a] Department of Biomedical Engineering and Biotechnology, University of Massachusetts Lowell, Lowell, MA 01854, United States
[b] Department of Chemical Engineering, University of Massachusetts Lowell, Lowell, MA 01854, United States
[c] Department of Chemical and Biomolecular Engineering, University of Delaware, Newark, DE 19713, United States

ARTICLE INFO

Keywords:
Gene therapy
Synthetic biology
RAAV production
Stable packaging cell line
Inducible circuit design
CRISPR-Cas9 site-specific integration

ABSTRACT

AAV-mediated gene therapy is a quickly growing segment of the pharmaceutical market; however, the current transient transfection process to produce rAAV has several challenges. The stable cells are ideal for large-scale continuous production, overcoming the drawbacks in the current transient transfection and streamlining rAAV production. In this study, we proposed to use synthetic inducible promoters to control the viral component expression and develop the baseline of HEK293T stable cells via site-specific integration mediated with CRISPR-Cas9, targeting safe harbor sites of human genome (ROSA26, AAVS1, and CCR5 locus). With a total of three round integrations, stable cell pools were developed and evaluated at each round of integration. Single clones were further characterized for each integration round. Regarding the stable pools, the 5' and 3' junction PCR results confirmed the site-specific integration to each locus. The genome copy result showed that AAV components, including Rep78/68, E2A, E4orf6, Cap, and Rep52/40, were successfully integrated into the host cell genome. Genome and capsid titer after induction confirmed rAAV production for stable cell pools in each round. The packaging cell line (after 2nd round integration) was able to produce rAAV. However, it was observed that the genome titer was ten-fold lower than that of rAAV products done with triple plasmids transfection. The out-to-out PCR and qPCR assay results further confirm the site-specific integration. This research demonstrates the feasibility of developing the inducible stable cell line with the refactored viral vectors via a site-specific integration.

1. Introduction

The gene therapy is rapidly expanding within the pharmaceutical market; however, the transient transfection method for recombinant adeno-associated virus (rAAV) production faces numerous challenges such as low productivity of rAAV from host cells, difficult scalability of the rAAV production process, and high levels of impurities (e.g. empty/partial capsid) during production [1–3].

Developing stable cell lines that express AAV replication and packaging proteins will be very useful to ensure consistent and efficient viral vector production. However, numerous challenges still need to be overcome. A stable producer cell line requires the integration of not only the transgene, Rep and Cap genes for genome replication and encapsidation, but also helper genes that initiate the rAAV replication. The main barrier to establishing a stable cell line is the cytotoxicity induced by the continuous expression of rep and helper genes after integration. To meet the current and future demands of gene therapy products, developing an inducible stable cell line is a critical step for rAAV production.

Several inducible promoters have been reported to successfully control the expression of the most toxic protein Rep78/68 [4,5] and the adenovirus helper proteins E2A and E4 [6,7]. Recently, with the rapid advancements of synthetic biology, CEVEC Pharmaceuticals reported the development of producer cell lines through stable and sequential transfection of rAAV components controlled by Tet-inducible promoters using CEVEC's Amniocyte Production (CAP) cells and human embryonic kidney (HEK293) cells [8,9]. Regarding academic insight, Lee et al. constructed the inducible stable cell line using synthetic biology combined with the strategy of transposon random integration, wherein multiple inducible promoters were utilized to regulate the expression of different rAAV components [10]. Separate control over replication and packaging activities further allowed the manipulation and regulation of empty/full capsid ratio [10]. Those results demonstrate the feasibility of

* Correspondence to: 1 University Ave, Lowell, MA 01854, United States
E-mail address: seongkyu_yoon@uml.edu (S. Yoon).

https://doi.org/10.1016/j.bej.2024.109552
Received 20 August 2024; Received in revised form 17 October 2024; Accepted 28 October 2024
Available online 31 October 2024

using inducible systems and applying synthetic biology in generating stable rAAV packaging and producer cell lines.

Compared to the random integration strategy, site-specific integration allows the targeted integration of transgenes to pre-validated genome loci [11]. That can overcome fundamental problems in random integration, such as high clone variation, loss of transgene, and uncontrollable integration sites [12]. Furthermore, genomic safety harbors are regions of the human genome that allow stable expression of transgenes without affecting the host cells [13]. The genomic loci that are most extensively targeted in human cells are adeno-associated virus integration site 1 (AAVS1), C-C motif chemokine receptor 5 (CCR5), and reverse orientation splice acceptor 26 (ROSA26) [14]. These aforementioned loci are acceptable for research purposes, but the clinical application needs to be further validated.

In this study, synthetic inducible promoters were employed to regulate the gene expression of refactored viral components and develop the baseline of the HEK293T stable cells via site-specific approach targeting safe harbor sites of human genome (ROSA26, AAVS1, and CCR5 locus); however, the refactored rAAV Rep, Cap, and helper genes under the control of inducible Tet-on promoters result in low AAV productivity in the stable packaging cell lines. Additional optimization strategies, such as optimization of gene expression level and timing for vector production, mitigation of toxic genes, and improvement of knock-in efficiency in targeted sites for large insertions, are proposed to achieve high rAAV titer in the stable cell lines. Overall, this study represents a significant leap forward in the realm of establishing stable cell lines for AAV production, although there are still numerous limitations and challenges, leaving plenty of room for future improvement.

2. Materials and methods

2.1. Vector design and plasmids construction

sgRNA-Cas9 plasmid construction: The sgRNA sequences targeting the ROSA26, AAVS1 and CCR5 locus were designed based on a prior publication [15], annealed, and then integrated into the sgRNA-Cas9 backbone plasmid (pU6-(*Bbs*I)_CBh-Cas9- T2A-mCherry) using golden gate assembly.

Donor plasmid construction: Homology arms were amplified via PCR from donor backbone plasmids (AAVS1-eGFP donor, ROSA26-eGFP donor, and CCR5-eGFP donor, gift from KAIST) [15,16]. The components of the AAV were generated either through synthesis by Twist Bioscience or PCR cloning from corresponding plasmids. Subsequently, they were assembled according to the vector design depicted in Fig. 1b using the golden gate assembly method. Then the homology arms sequences, selection genes, and well-prepared AAV components were assembled using NEBuilder HiFi DNA Assembly master mix (New England Biolabs, United States) followed by transformation using E. coli DH5α competent cells. Plasmids were verified by sequencing and prepared with the EndoFree plasmid maxi kit (Zymo, United States), according to the manufacturer's instructions. The information on the sgRNA sequences, donor sequences for AAVS1, ROSA26, and CCR5 loci, plasmids, and primers used in cloning is listed in Tables S1−S3.

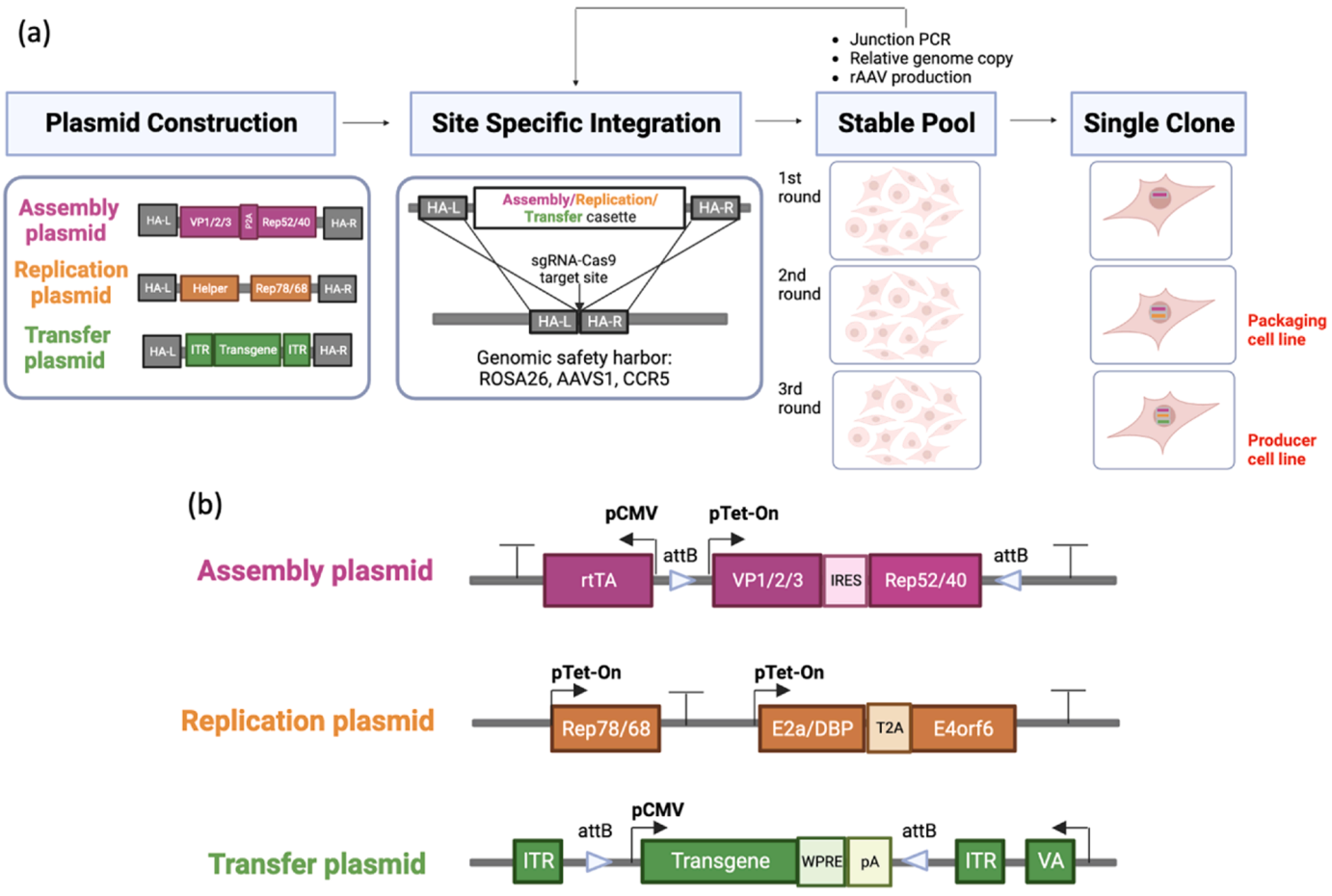

Fig. 1. (a) Workflow and (b) vector design. Three viral cassettes, including assembly, replication, and transfer cassettes, were constructed and integrated into three different genomic safety harbor sites sequentially via site-specific integration methods. Several assessment criteria, such as junction PCR, genome copy number, and rAAV productivity, were employed to evaluate the established stable cell pools, and single clones for the 2nd and 3rd rounds were fully characterized as packaging cell lines and producer cell lines. More details can be found in the result sections.

2.2. Cell culture, stable transfection, and single clone isolation

HEK293T/17 (ATCC, CRL-11268) cells were grown in Dulbecco's modified Eagle's medium (DMEM) (Gibco, United States) supplemented with 10 % fetal bovine serum (Gibco, United States). The cells were cultured in T-flasks (GenClone, United States) with a working volume of 5 mL at 37 °C under 5 % CO_2 and passaged every 4 days. To establish stable cell pools, we transfected donor and sgRNA-Cas9 vectors targeting safety harbor sites at a 1:1 (w:w) using Lipofectamine 2000 (Invitrogen, United States) followed by 2 weeks of selection with antibiotics: 5ug/mL blasticidin (InvivoGen, United States), 200ug/mL zeocin (InvivoGen, United States), and 2 μg/mL of puromycin (Sigma-Aldrich, United States). The viable cell density (VCD) and cell viability were assessed using a Nova Flex2 Analyzer (Nova Biomedical, United States). The single-cell clones were isolated from the stable pools using an MA900 cell sorter (Sony, Japan) and seeded individually into 96-well plates.

2.3. Genomic DNA extraction for junction PCR & copy number analysis

Site-specific integration of the target gene was evaluated using 5′ and 3′ junction PCR and out-to-out PCR was utilized for further confirmation [17,18]. The cell pellets from stable pools were collected for genomic DNA extraction. Genomic DNA was extracted from stable cell pools using Quick-DNA Miniprep Plus Kit (Zymo, United States) following the manufacturer's instructions. Approximately 100 ng of extracted DNA was used as the template for junction PCR, as described below. For single-cell clones [17], DNA was isolated by adding 20 μL of Quick-Extract DNA extraction solution when cells were confluent in 96 well plates. The mixture was then incubated at 65 °C for 15 min, followed by 5 min incubation at 98 °C. Of this mixture, 2 μL were used as the template for junction PCR, as described below. The 5'/3' junction PCR was performed using PrimeSTAR HS Premix (Takara Bio, Japan) by touchdown PCR (98 °C for 3 min; 10╳: 98 °C for 10 sec, 65 °C-55 °C (–1°C/cycle) for 30 sec, 72 °C for 2 min; 30╳: 98 °C for 10 sec, 55 °C for 30 sec, 72 °C for 2 min; 72 °C for 10 min.). The primer sequences used for the 5'/3' junction PCR are listed in Table S3.

For relative genome copy number analysis, qPCR was performed on genomic DNA samples using SYBR Green qPCR Master Mix (Thermo, United States) on the Bio-rad system (Biorad, United States). According to the manufacturer's instructions, qPCR reaction mixtures contained 2X SYBR Green master mix, 400 nM of forward and reverse primers, 20 ng of genomic DNA, and up to 20uL molecular biology water. Amplification was executed with the following conditions: 50 °C for 1 min; 95 °C for 10 min; 40 cycle: 95 °C for 15 s, 60 °C for 30 s, 72 °C for 1:30 min. The primer sequences used for Cap, Rep52/40, Rep78/68, E2a, E4orf6, codon-optimized green fluorescent protein (GFP), and glyceraldehyde 3-phosphate dehydrogenase (GAPDH) are listed in Table S3.

2.4. RNA isolation for gene expression evaluation

The gene expression assay, including RNA isolation, cDNA reverse transcription and gene expression by RT-PCR, was previously described [3]. The comparative cycle threshold ($2^{-\Delta\Delta Ct}$) method was used to analyze the transcript level fold changes between different conditions, in this case the induction of different doxycycline (dox) concentrations. The primer sequences used for the Cap, Rep52/40, Rep78/68, E2a, E4orf6, codon-optimized GFP, and GAPDH assessment are listed in Tables S3.

2.5. rAAV vector production, rAAV preparation and analytical methods (genome titer, capsid titer)

Triple plasmid transfection was performed for rAAV production. Three AAV-related plasmids were used, sourced from Addgene: pAd-DeltaF6, pAAV2/2, and AAV-CMV-GFP. Plasmid information is listed in Table S2. Cells in the logarithmic growth phase were seeded at a density of 5×10^5 cells per well in a 6-well plate. After a 24-hour incubation, transfection for stable pool evaluation was performed following the PEIpro manufacturer's instructions (Polyplus, United States), and the optimal condition of transfection obtained from the literature was utilized for single clone evaluation [19–21]. Specific transfection conditions can be found in Tables S4 and S5 of the Supplementary material.

After 68 hours post-transfection, harvested cell cultures were aliquoted to 1 mL volume (cells and supernatant inclusive) in 1.5 mL centrifuge tubes either for immediate analysis or stored at −80°C for future analysis. The genome titer and capsid titer assays followed the previously published paper [2].

2.6. Statistical analysis

GraphPad Prism 9 was used for processing raw data and statistical analysis. The workflow diagram and vector design were made in Biorender.

3. Results

1. Strategy and workflow

   We aimed to utilize CRISPR-Cas9 technology to accomplish site specific integration of refactored viral components and develop a stable cell line that can be induced for rAAV production in HEK293T cells, serving as the baseline for HEK293 stable producers. Fig. 1(a) shows the integration strategy and workflow. To achieve this goal, three essential viral cassettes were first constructed, including the assembly cassette, the replication cassette, and the transfer cassette. Detailed information about the components of each cassette can be found in the vector design section. Three cassettes were integrated into three different genomic safety harbors (ROSA26, AAVS1, and CCR5) respectively and sequentially. The first round of a stable pool was generated after the stable integration of the assembly cassette and corresponding antibiotic selection. As intermediate checkpoints, this stable pool was evaluated by junction PCR for targeted integration at the ROSA26 locus, relative genome copy analysis of assembly components, and its capability to produce AAV with two other plasmids transfection. Once the results met those criteria, the stable cell pool was maintained for the single clonal screening and the next round of the integration to expedite the overall integration process. The same integration and assessment process was applied to the replication and transfer cassettes targeting AAVS1 and CCR5 locus. The isolated single clones with intact target integration units in the specific sites after the second round of integration were further characterized as packaging cell lines. Similarly, the single clones with correct integrations after the third-round integration were then assessed as producer cell lines.
2. Vector design and construction

   The AAV production required components, including Rep (Rep78/68, Rep52/40), Cap, Helper genes (E2A/DBP, E4orf6, VARNA), and the Gene of Interest (GoI) flanked by ITR, were refactored into three different cassettes based on the function of different viral components [10]. The detailed information for the assembly, replication, and transfer cassettes is shown in Fig. 1(b) and Figure S1. (1) The assembly cassette includes the Cap gene and Rep52/40 gene, both crucial for capsid assembly and packaging. These two genes are regulated under a tet-on inducible promoter and linked by an internal ribosome entry site (IRES). IRES can effectively mitigate the cytotoxic effects of Rep52/40 expression by reducing its transcript level. The cassette also contains attB recombinase sites that allow the convenient switch between serotypes. Tetracycline-controlled transactivator repressor (rtTA) encodes proteins that regulate the expression of the gene of interest under the transcriptional control of the tetracycline-responsive promoter element (TRE). (2) The replication cassette comprises two tet-on inducible switches: one controls Rep68/78 expression, and another one controls E2a/DBP and

E4orf6. Minimum required viral helper components (DBP, E4orf6) are included in this cassette to reduce their cytotoxicity. (3) The transfer cassette contains ITR flanked GFP, and another helper gene VA RNA. The inclusion of attB recombinase sites enables the easy transgene switch in the future.

3. Stable pool evaluation for each round

Assembly, replication, and transfer cassettes were sequentially integrated to their corresponding target genomic safety harbor sites. After 2 weeks of antibiotic selection, the stable pool generated in each round was carefully evaluated. Genomic DNA was extracted from the stable pool. The targeted integration of each cassette in a designated locus was verified by 5'/3' junction PCR. The relative genome copy number of integrated cassettes in the stable pool was further measured by qPCR assay. Lastly, the stable pool in each round was transiently transfected for rAAV production to assess the effect of integration on cassette expression and its functionality. To be more specific, transient transfection with three donor plasmids containing refactored viral components serves as donor control (DC). The first-round stable pool was transient transfected with the remaining two donor plasmids for rAAV production, and the second-round stable pool was transient transfected with transfer donor plasmid only. 5 μg/mL dox was added for all the conditions to induce gene expression and vector production [10]. Genome and capsid titer were used to evaluate the rAAV production.

After each round of integration, 5′/3′ junction PCR was conducted to confirm the target integration in the stable cell pool. The gel image confirmed the integration of the assembly cassette in the first-round stable pool and the integration of the replication cassette in the second-round stable pool (Data not shown). The gel electrophoresis image (Fig. 2a) displayed the junction PCR results of the stable pool after the third round of integration, and the results affirmed the successful integration of all three cassettes at their intended target sites.

The relative gene copy numbers of viral components, including Cap, Rep52, Rep68, DBP, E4orf6, and transfer cassette (GFP), were assessed through qPCR assays after each round of integration, with GAPDH serving as the internal reference. As indicated in Table 1, copy numbers of housekeeping gene GAPDH remained consistent across all three stable cell pools and negative control (NC)/parental cells. In comparison to the NC group, the Cq values for viral components were below 29 in the stable cell pool after each round of integration, indicating the detection and successful integration of each viral component into the host cell genome.

To further assess the stable integration process, transient transfections with unintegrated donor cassettes were performed as intermediate checkpoints. The genome titer (Fig. 2b) and capsid titer (Fig. 2c) after 68 hours of induction with 5 μg/mL dox were utilized to evaluate rAAV productivity. In general, the genome titer after the 1st (2.32E+11 vg/L) and 2nd (2.77E+11 vg/L) round of integrations were comparable to that of the donor control (3.18E+11 vg/L), but no genome titer was detected after the 3rd round. Similarly, the capsid titer after the 1st (3.04E+11 cp/L) and 2nd (3.05E+11 cp/L) integrations was comparable to that of the donor control (3.01E+11 cp/L). Although the amount of capsids in the 3rd round of integration was detectable (8.32E+10 cp/L), there was a significant decrease compared to the amount in donor control, 1st, and 2nd round stable cell pools. In general, the genome titer and capsid titer confirmed the production of rAAV with refactored donor plasmids and the effective integration of viral components into the host genome. The detection of capsids after the 3rd round of integration confirmed capsid production. However, it was important to notice the absence of genome titer when utilizing the 3rd round stable pool to produce rAAV. This might result from inadequate viral replication due to the low transgene copy numbers compared to those achieved in transient transfection. Together with limited viral proteins production, the relatively low packaging efficiency, an inherent barrier in rAAV production, further contributes to the undetectable genome titer [22]. Such observation underscores the need to integrate multiple copies of transgene and cap-encoding plasmids to enhance

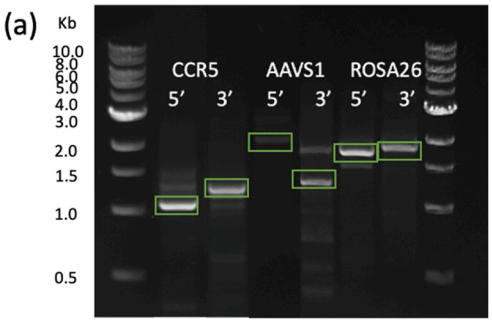

Lane	Sample	Expected size
1	Ladder	N/A
2	CCR5 5' junc	1120 bp
3	CCR5 3' junc	1379 bp
4	AAVS1 5' junc	1928 bp
5	AAVS1 3' junc	1288 bp
6	ROSA26 5' junc	1784 bp
7	ROSA26 3' junc	1932 bp
8	Ladder	N/A

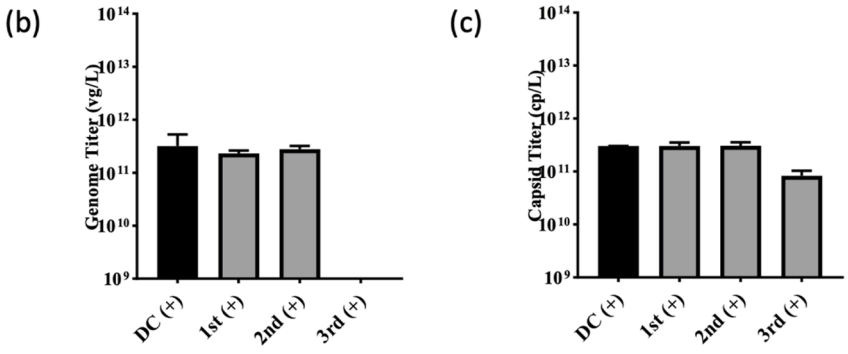

Fig. 2. (a) Junction PCR results for the stable cell pool after three rounds of integration. The sample names and expected sizes are shown in the right table. The green boxes in the gel image show the corresponding bands in the expected size. AAV production evaluation for each round of stable pool with 5 μg/mL dox induction (+). Donor control (DC) represents the transient transfection process with three re-constructed donor plasmids. Data represent the mean and standard deviation of biological duplicates (n=2). (b) Genome titer in vg/L harvest at 68 hours after transfection (HPT). (c) Capsid titer in cp/L at 68 HPT.

Table 1
Relative genome copy analysis summary of viral components for stable cell pools after each round of integration.

Relative genome copy	House keeping	Assembly cassette		Replication cassette			Transfer cassette
n=3	GAPDH	Cap	Rep52	Rep68	DBP	E4orf6	GFP
293TAssrtTA RepTrans (3rd)	24.47± 0.21	23.4±0. 73	25.06± 1.11	26.17± 0.17	24.81± 0.1	25.25± 0.1	22.92± 0.05
293TAssrtTA Rep (2nd)	24.94± 0.35	23.66± 0.13	22.69± 0.17	26.08± 0.25	25.27± 0.14	25.17± 0.18	
293TASSrtT A (1st)	23.88± 0.11	24.86± 0.03	23.68± 0.04				
NC	24.04± 0.06	34.92± 0.47	35.4±0. 43	37.93± 2.18	38.0± 1.93	30.1± 0.25	34.83± 0.41

Footnote: The data here represent the mean and standard deviation of biological triplicates (n=3). NC represents negative control/parental cells. rtTA represents tet-on inducible promoter.

overall productivity [22,23]. Stable cell pools after each round of integration were then maintained for single clone screening.

4. Knock-in efficiency results

Approximately 30–70 single clones were isolated and screened from each round of stable cell pools. Two criteria were defined: site-specific integration with positive 5'/3' junction PCR results; and detection of all the viral components in the host cell genome via relative genome copy assay. Any clones in the 2nd and 3rd rounds that passed the two criteria were further explored and fully characterized for rAAV production.

Table 2 shows the summary of junction PCR screening results for targeted integration and the gel electrophoresis image of junction PCR screening is shown in Figure S2. Out of 55 clones picked from 1st round stable pool, 3 clones were 5'/3' junction (ROSA26) positive. Out of 38 clones from 2nd round stable pool, 2 clones were 5'/3' junction (AAVS1) positive. Out of 62 clones from 3rd round stable pool, 12 clones were 5'/3' junction (CCR5) positive. It was observed that with the larger insertion size, CRISPR-Cas9 mediated knock-in efficiency tends to be lower. Further explanation can be found in the discussion.

Clones with targeted integration were further assessed for their genome copy of viral components. Table 3 shows the relative genome copy of all the required viral components for the 1st round single clones (Cap and Rep52) and the 2nd and 3rd single clones (Cap, Rep52, Rep68, DBP, and E4orf6). Genome copy results for stable cell pool were listed again at the end of each table here for comparison. According to the Cq value of viral components in the NC group (Cq >30), any viral components in single clones with genome copy Cq value greater than 29 were defined as missing. Overall, 2 clones out of 3 had Cap and Rep52 successfully integrated in the first round, 2 clones out of 2 had all viral components integrated for the second round, and no clones had all the components detected after 3rd round integration, either missing Rep or Cap genes. The observations, such as the small number of single clones isolated and the missing gene components for each round, will be further explored in the discussion. Single clones picked up after 2nd round of integration were evaluated and fully characterized as the packaging cell lines in the next section.

5. Single clone evaluation (packaging cell line)

Single clone 4-7 in the 2nd round was selected and fully characterized as the packaging cell line. The relative transcript level of viral genes in the packaging cell 4-7 after induction was measured by qPCR assay. Different dox concentrations, 0 μg/mL, 0.5 μg/mL and 5 μg/mL were added to induce the gene expression (Fig. 3/Table 4). Detected signals of viral components at 0 μg/mL induction shown in Table 4 indicated the leakage of the designed inducible promoter. The extent of leakiness varied among the genes. Despite being constructed within the same vector, DBP exhibited the lowest degree of expression leakage compared to Rep68 and E4orf6. The variations in transcript level and the extent of leakage could potentially relate to different primer amplification efficiencies and promoter interference [24]. Addition of 0.5 and 5 μg/mL dox were both able to induce the viral gene expressions. The fold change of transcript level in 0.5 and 5 μg/mL doxycycline relative to that 0 μg/mL dox was shown in Fig. 3. The trend further confirmed that 5 μg/mL dox can be used to maximize gene expression for later rAAV production. The transcript levels (Cq values) for Rep68, DBP, and E4orf6 following 5 μg/mL dox induction were comparable, suggesting the consistent expression from the same cassette. Compared with the Cap gene, the higher transcript level of Rep52 at 0 and 5ug/mL dox might result from the potential leakage expression of Rep68, although the p19 promoter was mutated to prevent any Rep52 synthesis from the replication cassette. Transcript levels of Rep and helper genes were elevated to a great extent as expected after the addition of dox. The transcript level of the Cap gene showed a roughly two-fold increase after induction, but this increase was comparatively lower than the changes in expression levels observed in other viral genes at 0 and 5 μg/mL dox induction. This suggests the need for further optimization of the inducible system.

Packaging cell line 4-7 was transfected with transfer donor plasmid for rAAV production. Cell cultures induced with 5 μg/mL dox and uninduced (0 μg/mL dox) cell culture were compared in parallel to understand the extent of promoter leakage. Positive control, traditional triple transient transfection with commercial plasmids (Addgene), and donor control (transient transfection with refactored donor plasmids) were used as the reference for later optimization of rAAV productivity in inducible stable cell lines. Fig. 4 demonstrated that compared to positive control, donor control resulted in approximately 10-fold lower genome titer (Fig. 4a) and 100-fold lower capsid titer (Fig. 4b), indicating spacious room to improve productivity based upon the optimization of inducible system and vector design. Packaging cell line SC4-7 was expected to have no titer at 0 μg/mL dox induction. Sensitivity of qPCR

Table 2
Knock-in efficiency summary for three rounds of integrations.

Integration Round	Locus Targeted	Insertion Size	Isolated Single Clones	One Junction PCR	5' & 3' Junction PCRs	Knock-in Efficiency
1st	ROSA26	8653	55	17	3	~ 5.5 %
2nd	AAVS1	8397	38	20	2	~ 5.2 %
3rd	CCR5	5982	62	24	11	~ 17.7 %

Table 3
Genome copy analysis summary for isolated single clones from each stable cell pool.

Relative genome copy	House keeping	Assembly cassette		Replicaton cassette		
n=3	GAPDH	Cap	Rep52	Rep68	DBP	E4orf6
1st sc2-2	24.43±0.11	25.34±0.08	23.17±0.02	NA	NA	NA
1st sc2-1	23.68±0.15	24.35±0.2	31.74±0.77	NA	NA	NA
1st sc4-5	24.23±0.09	24.47±0.04	22.79±0.28	NA	NA	NA
1st stable pool	23.88±0.11	24.86±0.03	23.68±0.04	NA	NA	NA
2nd sc3--2	24.42±0.04	21.5±0.07	21.49±0.08	21.06±0.03	21.45±0.05	19.64±0.07
2nd sc4-7	24.53±0.3	21.58±0.02	21.35±0.14	20.97±0.05	22.19±0.01	20.1±0.07
2nd stable pool	24.94±0.3	23.66±0.02	22.69±0.14	26.08±0.05	25.27±0.01	25.17±0.07
3rd sc2-4	24.4±0.33	29.97±0.36	25.86±0.31	30.4±0.14	25.03±0.02	29.73±0.09
3rd sc2-6	24.85±0.27	29.61±0	26.14±0.01	29.59±0.42	25.67±0.34	29.63±0.16
3rd sc2-14	24.25±0.28	30.37±0.14	25.58±0.15	30.31±0.21	25±0.14	29.53±0.5
3rd sc3-9	24.56±0.13	30.02±0.48	26.1±0.01	29.75±0.33	25.23±0.02	29.37±0.28
3rd sc5-6	24.7±0.12	29.63±0.17	29.7±0.03	30.1±0.04	26±0.03	29.73±0.12
3rd sc1-6	24.28±0.04	30.44±0.09	30.43±0.2	30.83±0.26	25.69±0.27	30.03±0.16
3rd sc1-7	23.98±0.12	30.31±0.4	25.3±0.1	31±0.14	24.53±0.05	30.08±0.28
3rd sc1-16	24.72±0.08	30.13±0.14	25.15±0.03	30.45±0.3	25±0.45	30.22±0.24
3rd sc4-13	23.81±0.17	30.47±0.87	30.83±0.94	31.14±0.97	24.95±0.33	29.96±0.37
3rd sc4-15	23.78±0.05	30.36±0.02	30.94±0.39	31±0.04	25.23±0.08	29.84±0.28
3rd sc4-17	24.77±0.08	30.04±0.39	26.05±0.02	30.61±0.14	25.37±0.04	30.2±0.36
3rd stable pool	24.47±0.21	23.4±0.73	25.06±1.11	26.17±0.17	24.81±0.1	25.25±0.1

Footnote: Red highlight represents the missing of corresponding viral genes. Green highlight means the isolated single clones have all the components integrated and can be confirmed by genome copy analysis.

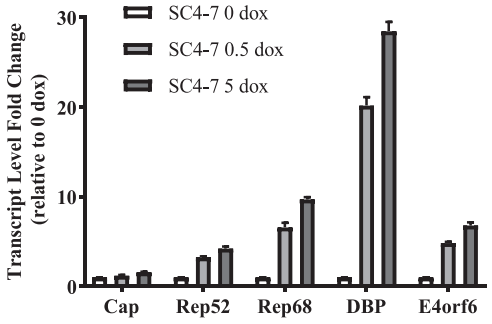

Fig. 3. Transcript level of viral genes fold change with 0, 0.5, and 5 μg/mL dox induction at 68 HPT for packaging single clone (SC4-7), normalized to house-keeping gene GAPDH. Key viral components include Cap, Rep52, Rep68, DBP, and E4orf6. Presented numbers for dox represent the actual concentration of inducers used in μg/mL. Data represent the mean and standard deviation of triplicate wells (n=3).

titer assay and leakage of the designed inducible system can be potential reasons for the SC4-7 0 dox genome titer result shown in Fig. 4a. With the addition of 5 μg/mL dox, genome titer for SC4-7 (8.46E+11 vg/L) was slightly lower than that for donor control (1.15E+12 vg/L); whereas capsid titer (8.79E+10 cp/L) was 3-fold lower than that for donor control (2.58E+11 cp/L). The big variation between genome and capsid titer might result from the sensitivity and limitations of each assay in the low titer profile.

The genome titer variation at 0 and 5 μg/mL dox induction was overall consistent with the transcript level changes of viral components. Low genome titer at 0 dox induction suggested that the leaky expression

Table 4
Transcript Cq value summary of all the viral components in the single clone packaging cell line SC4-7 with 0, 0.5, 5 μg/mL dox induction via RT-PCR assay.

Transcripts	House keeping	Assembly cassette		Replicaton cassette		
	GAPDH	Cap	Rep52	Rep68	DBP	E4orf6
sc 4–7 0 dox	17.86 ±0.05	23.03 ±0.04	21.23 ±0.08	24.07 ±0.06	25.19 ±0.07	22.38 ±0.1
sc 4–7 0.5 dox	17.91 ±0.06	22.61 ±0.05	19.32 ±0.07	21.13 ±0.07	20.63 ±0.02	19.85 ±0.06
sc 4–7 5 dox	17.64 ±0.04	22.17 ±0.05	18.94 ±0.06	20.57 ±0.01	20.14 ±0.04	19.39 ±0.05

of viral components was not sufficient to support rAAV replication. After the addition of 5 μg/mL dox, there was a noticeable increase in genome titer together with the increase in transcript levels. However, there was a slight discrepancy observed in capsid titers. With only 2-fold difference in Cap gene transcript levels (Fig. 3), the capsid titer was undetectable at 0 μg/mL dox induction but became detectable at 5 μg/mL dox induction. The Cap expression in 0 dox condition was largely due to the leakiness of the designed promoter, but incorrect VP stoichiometric ratio and improper assembly process potentially resulted from insufficient expression of other rAAV viral components might lead to the capsid titer lower than the detection limit. Overall, the performance in the transcript level, genome titer, and capsid titer confirmed that this cell line was able to produce rAAV, although the productivity was significantly lower than that in traditional triple transfection. The potential optimization strategies will be depicted in the discussion.

Site-specific integration was further confirmed by out-to-out PCR (Figure S3). Due to the large insertion size, two pairs of primers were designed to separately amplify left (5') and right (3') insert fragments

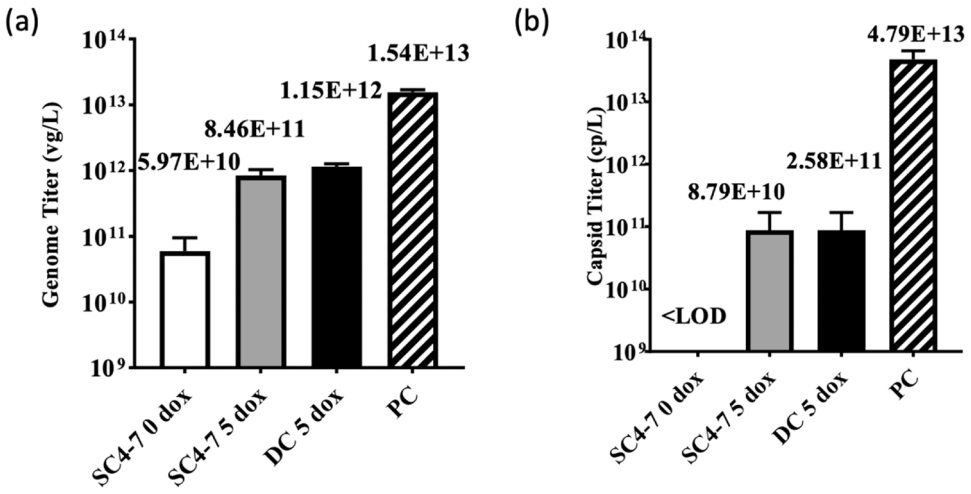

Fig. 4. Genome titer (a) and capsid titer (b) evaluation for packaging single clone SC4-7 with 0 and 5 μg/mL dox induction. Positive control (PC) represents traditional transfection with commercial triple plasmids. Donor control (DC) represents transfection with refactored donor plasmids with 5 μg/mL dox induction. LOD represents the lower limit of detection. Error bars represent the standard deviation of biological triplicates (n=3). Note: One data point for donor control and SC4–7 5 μg/mL dox was eliminated as an outlier for capsid titer measurement.

with 376 bp overlap. The primer design strategy is shown in Figure S3. PCR products were further purified and assessed for their relative genome copies of viral components via qPCR assay. This validated that Rep68, DBP, and E4orf6 was precisely integrated into the target locus AAVS1.

The cell growth performance and the cell line stability of the established packaging cell line were further evaluated, with results shown in Fig. 5. Regarding the cell growth performance (Fig. 5(a)), both parental

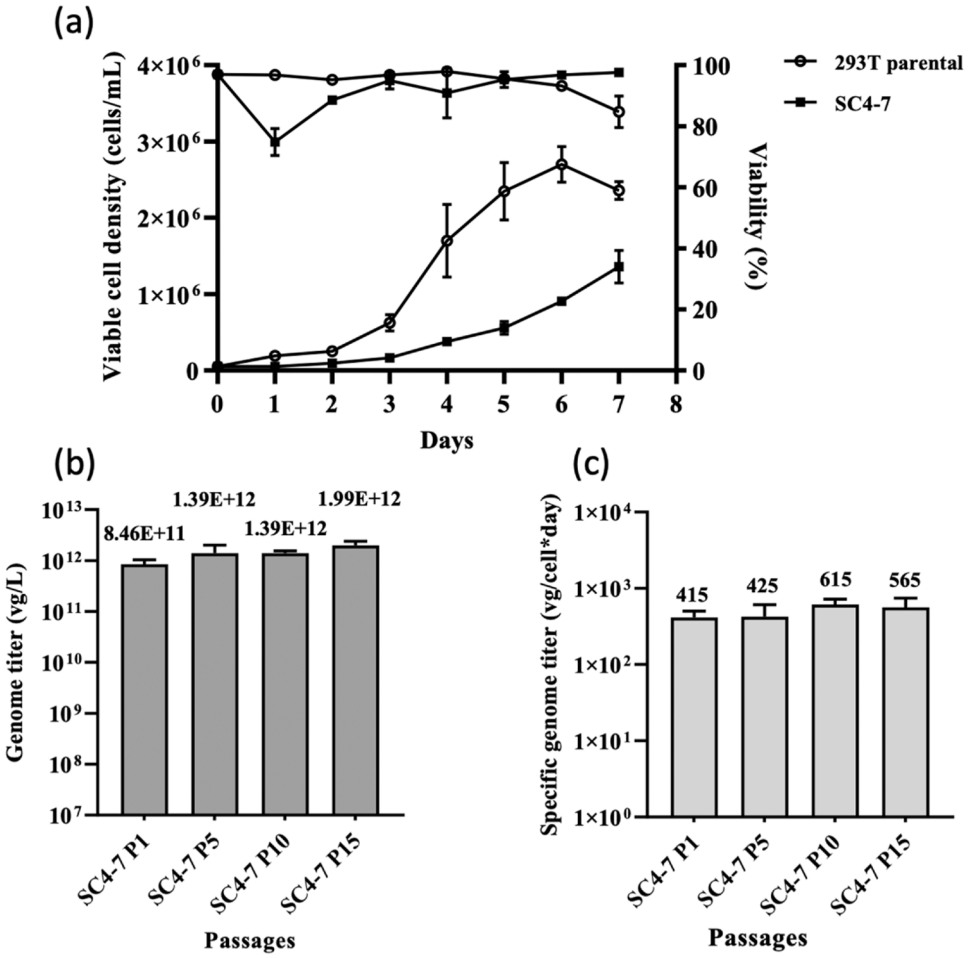

Fig. 5. Cell growth performance (a) and cell line stability (b & c) evaluation for packaging single clone SC4-7. In Fig. 5(a), the bottom two curves represent viable cell density, while the top two curves depict cell viability. Error bars represent the standard deviation of biological triplicates (n=3).

and packaging cell line were plated at the same initial density (5E4 cells / well) in 12-well plates. Daily viable cell density (VCD) and viability were monitored over 7 days. SC4–7 exhibited much slower growth rate compared to 293 T parental cells, with notably lower viability. The slower growth of SC4–7 demonstrated potential leakiness in the expression of viral components, leading to cytotoxicity. As for the cell line stability (Fig. 5(b & c)), isolated single clone was maintained for over 15 passages. The genome titer was assessed every five passage to evaluate the stability of the cell line. The results showed that the titer was comparable, achieving a similar order of magnitude through 15 passages.

4. Discussion

The goal of this study is to establish the baseline of an inducible stable cell line for rAAV production with site-specific integration. High expression levels of viral components, such as Rep and helper genes, and cytotoxicity associated with these components were the challenges in constructing stable cell lines for viral vectors. With the design of an inducible circuit, it can effectively regulate the level of gene expression. Additionally, site-specific integration allows the targeted integration of transgenes to pre-validated genome loci [11]. In contrast to the widely used random integration method for generating stable monoclonal antibody production in CHO cells, this approach necessitates less time-consuming isolation and screening of clones to obtain stable high producers [11,25].

We were able to isolate several 293 T clones as packaging cell lines and fully characterize the established stable cell line. In the selected single clone 4–7, at least one copy of each viral component was detected. With the addition of the inducing reagent, the transcript levels of the integrated viral components were significantly boosted. It can result in genome titer 8.46E+11 vg/L and capsid titer 8.79E+10 cp/L. The site-specific integration was confirmed by 5'/3' junction PCR and out-to-out PCR for replication cassette targeting the AAVS1 locus.

The proof of concept for developing a stable AAV cell line in this study was demonstrated by the characterized packaging cell line. This involved redesigning viral components and regulating them with inducible promoters, along with using site-specific integration methods. However, there are several inherent limitations expected for this study: overall low knock-in efficiency for CRISPR-Cas9 mediated large fragment insertion; low genome titer resulting from refactoring of viral components; and promoter leakage and inducibility.

Low knock-in efficiency and potential strategies to improve: Approximately 400–500 single clones were isolated from stable cell pools in each round initially. Only 30–60 clones were able to survive and grow. Out of these viable clones, only 5 % of clones had inserts successfully integrated into the target loci. This observation aligns with the reported challenges and limitations of existing CRISPR-Cas9 technology, including low knock-in efficiency, which is even more problematic with larger inserts (greater than 3000 bp) in mammalian cell lines [26,27]. Double strand break (DSB) induced by active Cas9 can be repaired by two major pathways: non-homologous end joining (NHEJ) and homology directed repair (HDR). Targeted integration utilizes CRISPR/Cas9 and HDR to precisely insert transgenes containing homology arms (HA) into the desired locus. NHEJ is one of the fastest and an active repair pathway existing in almost all the cell cycle phases, whereas HDR is primarily active in G2/S phase [28]. Low HDR efficiency became the major reason for relatively low knock-in efficiency. This might also explain why important viral components integrated earlier were lost for the majority of isolated producer clones, after three rounds of integration and selection process. It is also worth noting that both HEK293 and 293 T cells were initially used for stable cell line development. After integrating the replication cassette in the second round, the HEK293 stable cell pool encountered a loss of integrated assembly components (data not shown). Consequently, HEK293 was discontinued, and we proceeded with 293 T cells. Thus, to develop stable cell lines in the future, it is essential to increase HDR efficiency for site-specific integration. Several strategies have been attempted and developed in different models, such as adding small molecules to inhibit NHEJ pathways [29–32], controlling cell cycles to keep cells in HDR rich S/G2 phase [33–35], enriching the donor near Cas9-induced DSB [33–35], and co-expressing DNA repair protein involved in HDR [36,37]. These strategies can be applied and explored in future studies.

Low genome titer and future directions to optimize: In this study, rAAV Rep, Cap, and helper genes were refactored and regulated under three inducible Tet-on promoters. The genome titer obtained by transient transfection with refactored donor plasmids was significantly lower than that by traditional transient transfection with commercially available plasmids. With the same viral gene sequences, the low titer in donor control indicates the potential for optimization and improvement in inducible systems. In our scenario, we only utilized Tet-on inducible promoter with a total number of three to separately control the different viral components. The use of one type of Tet-on inducible promoter simplifies the production process by minimizing the addition of various inducible reagents [10]; however, the modulation of gene expression levels and timing for diverse viral components to achieve optimal production demands becomes challenging. To better regulate the gene expression level and timing, the inducible promoters can be tuned by the number and the spacing between of tetO sites [38–40]. Protein expression control can be achieved by screening Kozak sequence variants and modulating the translational efficiency [41,42]. Various factors in circuit designs, such as inducibility, leakage, control of gene expression, and expression timing, can be screened and evaluated during transient transfection. The inducible system can be adjusted to achieve maximum productivity and optimal quality before progressing to stable integration.

The cytotoxicity associated with viral components remains a challenge in stable cell line development. In our case, we found that the cells in stable pools after the second round of integration and packaging cell line SC4-7 grew much slower than parental cells. Moreover, the transcript data revealed detectable levels of all viral components in the packaging cells at 0 μg/mL dox induction, indicating the leakage of the designed inducible circuit. We attribute the low cell growth rate in the stable pools and packaging cell line to the leaky expression of the toxic genes, particularly the Rep78. Rep78 has been shown to activate caspase-3 and induce cell apoptosis [43], decrease Cdc25A activity, and block the cell cycle in the S phase [44]. Therefore, we hypothesize that the leakage of these toxic genes could significantly impact cell physiology, thereby potentially impeding AAV production. In future studies, additional regulations, such as the use of a second inducible circuit [1] can be proposed to tightly control the expression of those toxic genes. In addition, the literature reported that a conditional degron tag can be used to modulate protein stability and regulate protein expression at the post-translational level [45]. Therefore, the degron tag can be used in the future to tune Rep78/68 lifetime, regulate its degradation, and eliminate the cytotoxicity associated with it. Furthermore, the mechanistic study of the cytotoxicity associated with Rep genes and helper genes from the host cell perspective [46,47], such as utilizing omics and CRISPR-Cas9 genome wide screening tools, will also be necessary and useful for rational modifications to enhance the tolerance of the host cells.

5. Conclusion

In conclusion, this study successfully established an inducible stable packaging cell line for AAV production through a site-specific integration strategy. The introduction of the inducing reagent resulted in a significant increase in transcript levels of integrated viral components, yielding a genome titer of 8.46E+11 vg/L and a capsid titer of 8.79E+10 cp/L. Site-specific integration was confirmed through junction PCR and out-to-out PCR. The successful characterization of the isolated inducible packaging cell line indicates the potential of developing stable producer

cell lines in the future. Efforts can be focused on the improvement of transgene cassette copy numbers. Additionally, addressing challenges such as low knock-in efficiency, optimizing gene expression levels, and timing for various viral components, and minimizing the leakage of toxic genes can further help achieve the goal of the inducible rAAV high producing stable cell line.

Ethical statement

This article does not contain any studies with human participants or animals performed by any of the authors.

CRediT authorship contribution statement

Qiang Fu: Writing – original draft, Visualization, Methodology, Investigation, Funding acquisition, Formal analysis, Data curation, Conceptualization. **Yongdan Wang:** Writing – original draft, Visualization, Methodology, Investigation, Formal analysis, Data curation. **Emily Doleh:** Writing – review & editing, Methodology, Investigation, Data curation. **Mark Blenner:** Writing – review & editing, Supervision, Resources, Project administration, Funding acquisition, Formal analysis. **Seongkyu Yoon:** Writing – review & editing, Supervision, Resources, Project administration, Investigation, Funding acquisition.

Declaration of Competing Interest

The authors declare the following financial interests/personal relationships which may be considered as potential competing interests: Seongkyu Yoon reports financial support and travel were provided by University of Massachusetts Lowell. Seongkyu Yoon has patent Provisional Patent pending to N/A. N/A If there are other authors, they declare that they have no known competing financial interests or personal relationships that could have appeared to influence the work reported in this paper.

Acknowledgements

This work was funded and supported by the Advanced Mammalian Biomanufacturing Innovation Center (AMBIC) through the Industry–University Cooperative Research Center Program under the U.S. National Science Foundation (Grant number 2100075). We would like to express our gratitude to all AMBIC member companies for their mentorship and their financial support. This work was also partially funded by the Massachusetts Life Science Center (MLSC). We also would like to thank the plasmids gift from Dr. Gyunkim Lee lab in Korea Advanced Institute of Science & Technology (KAIST).

Appendix A. Supporting information

Supplementary data associated with this article can be found in the online version at doi:10.1016/j.bej.2024.109552.

Data availability

Data will be made available on request.

References

[1] Q. Fu, et al., Critical challenges and advances in recombinant adeno-associated virus (rAAV) biomanufacturing, Biotechnol. Bioeng. (2023).
[2] Q. Fu, et al., Design space determination to optimize DNA complexation and full capsid formation in transient rAAV manufacturing, Biotechnol. Bioeng. (2023).
[3] Y. Wang, et al., Transcriptomic features reveal molecular signatures associated with recombinant adeno-associated virus production in HEK293 cells, Biotechnol. Prog. (2023) e3346.
[4] Q. Yang, F. Chen, J.P. Trempe, Characterization of cell lines that inducibly express the adeno-associated virus Rep proteins, J. Virol. 68 (8) (1994) 4847–4856.
[5] C. Hölscher, et al., Cell lines inducibly expressing the adeno-associated virus (AAV) rep gene: requirements for productive replication of rep-negative AAV mutants, J. Virol. 68 (11) (1994) 7169–7177.
[6] D.E. Brough, et al., A gene transfer vector-cell line system for complete functional complementation of adenovirus early regions E1 and E4, J. Virol. 70 (9) (1996) 6497–6501.
[7] I. Kovesdi, S.J. Hedley, Adenoviral producer cells, Viruses 2 (8) (2010) 1681–1703.
[8] Hein, K., et al., *Generation of helper virus-free adeno-associated viral vector packaging/ producer cell lines based on a human suspension cell line.* 2018.
[9] K. Swiech, V. Picanço-Castro, D.T. Covas, Human cells: new platform for recombinant therapeutic protein production, Protein Expr. Purif. 84 (1) (2012) 147–153.
[10] Z. Lee, et al., Construction of an rAAV Producer Cell Line through Synthetic Biology, ACS Synth. Biol. 11 (10) (2022) 3285–3295.
[11] N.K. Hamaker, K.H. Lee, Site-specific integration ushers in a new era of precise CHO cell line engineering, Curr. Opin. Chem. Eng. 22 (2018) 152–160.
[12] J.S. Lee, et al., Mitigating clonal variation in recombinant mammalian cell lines, Trends Biotechnol. 37 (9) (2019) 931–942.
[13] J. Yu, et al., Human induced pluripotent stem cells free of vector and transgene sequences, Science 324 (5928) (2009) 797–801.
[14] G. Pavani, M. Amendola, Targeted gene delivery: where to land, Front. Genome Ed. (2021) 36.
[15] S. Shin, et al., Comprehensive analysis of genomic safe harbors as target sites for stable expression of the heterologous gene in HEK293 cells, ACS Synth. Biol. 9 (6) (2020) 1263–1269.
[16] D. Hockemeyer, et al., Efficient targeting of expressed and silent genes in human ESCs and iPSCs using zinc-finger nucleases, Nat. Biotechnol. 27 (9) (2009) 851–857.
[17] J.S. Lee, et al., Site-specific integration in CHO cells mediated by CRISPR/Cas9 and homology-directed DNA repair pathway, Sci. Rep. 5 (1) (2015) 8572.
[18] Z. Huang, et al., CRISPR-Cas9 mediated stable expression of exogenous proteins in the CHO cell line through site-specific integration, Int. J. Mol. Sci. 24 (23) (2023) 16767.
[19] J.C. Grieger, S.M. Soltys, R.J. Samulski, Production of recombinant adeno-associated virus vectors using suspension HEK293 cells and continuous harvest of vector from the culture media for GMP FIX and FLT1 clinical vector, Mol. Ther. 24 (2) (2016) 287–297.
[20] B. Gu, et al., Establishment of a scalable manufacturing platform for in-silico-derived ancestral adeno-associated virus vectors, Cell Gene Ther. Insights 4 (S1) (2018) 753–769.
[21] H. Zhao, et al., Creation of a high-yield AAV vector production platform in suspension cells using a design-of-experiment approach, Mol. Ther. -Methods Clin. Dev. 18 (2020) 312–320.
[22] M. Lu, et al., Enhancing the production of recombinant adeno-associated virus in synthetic cell lines through systematic characterization, Biotechnol. Bioeng. (2024).
[23] M. Lu, et al., Tuning capsid formation dynamics in recombinant adeno-associated virus producing synthetic cell lines to enhance full particle productivity, Biotechnol. J. 19 (3) (2024) 2400051.
[24] J. Curtin, et al., Bidirectional promoter interference between two widely used internal heterologous promoters in a late-generation lentiviral construct, Gene Ther. 15 (5) (2008) 384–390.
[25] S.W. Shin, J.S. Lee, CHO cell line development and engineering via site-specific integration: challenges and opportunities, Biotechnol. Bioprocess Eng. 25 (2020) 633–645.
[26] T.S. Nambiar, et al., CRISPR-based genome editing through the lens of DNA repair, Mol. Cell 82 (2) (2022) 348–388.
[27] K.M. Fichter, T. Setayesh, P. Malik, Strategies for precise gene edits in mammalian cells, Mol. Ther. -Nucleic Acids (2023).
[28] Z. Mao, et al., Comparison of nonhomologous end joining and homologous recombination in human cells, DNA Repair 7 (10) (2008) 1765–1771.
[29] C. Yu, et al., Small molecules enhance CRISPR genome editing in pluripotent stem cells, Cell stem Cell 16 (2) (2015) 142–147.
[30] V.T. Chu, et al., Increasing the efficiency of homology-directed repair for CRISPR-Cas9-induced precise gene editing in mammalian cells, Nat. Biotechnol. 33 (5) (2015) 543–548.
[31] F. Robert, et al., Pharmacological inhibition of DNA-PK stimulates Cas9-mediated genome editing, Genome Med. 7 (2015) 1–11.
[32] J. Song, et al., RS-1 enhances CRISPR/Cas9-and TALEN-mediated knock-in efficiency, Nat. Commun. 7 (1) (2016) 10548.
[33] P. Ruff, et al., Aptamer-guided gene targeting in yeast and human cells, Nucleic Acids Res. 42 (7) (2014) e61-e61.
[34] J. Carlson-Stevermer, et al., Assembly of CRISPR ribonucleoproteins with biotinylated oligonucleotides via an RNA aptamer for precise gene editing, Nat. Commun. 8 (1) (2017) 1711.
[35] B. Gu, E. Posfai, J. Rossant, Efficient generation of targeted large insertions by microinjection into two-cell-stage mouse embryos, Nat. Biotechnol. 36 (7) (2018) 632–637.
[36] L. Wang, et al., Enhancing targeted genomic DNA editing in chicken cells using the CRISPR/Cas9 system, PLoS One 12 (1) (2017) e0169768.
[37] B.S. Paulsen, et al., Ectopic expression of RAD52 and dn53BP1 improves homology-directed repair during CRISPR–Cas9 genome editing, Nat. Biomed. Eng. 1 (11) (2017) 878–888.
[38] S. Agha-Mohammadi, et al., Second-generation tetracycline-regulatable promoter: repositioned tet operator elements optimize transactivator synergy while shorter

minimal promoter offers tight basal leakiness. J. Gene Med.: A Cross-Discip. J. Res. Sci. gene Transf. its Clin. Appl. 6 (7) (2004) 817–828.
[39] R. Loew, et al., Improved Tet-responsive promoters with minimized background expression, BMC Biotechnol. 10 (2010) 1–13.
[40] M. Gossen, H. Bujard, Tight control of gene expression in mammalian cells by tetracycline-responsive promoters, Proc. Natl. Acad. Sci. 89 (12) (1992) 5547–5551.
[41] N. Blanco, et al., Tailoring translational strength using Kozak sequence variants improves bispecific antibody assembly and reduces product-related impurities in CHO cells, Biotechnol. Bioeng. 117 (7) (2020) 1946–1960.
[42] L. Xu, et al., Fine-tuning the expression of pathway gene in yeast using a regulatory library formed by fusing a synthetic minimal promoter with different Kozak variants, Microb. Cell Factor. 20 (2021) 1–11.
[43] M. Schmidt, S. Afione, R.M. Kotin, Adeno-associated virus type 2 Rep78 induces apoptosis through caspase activation independently of p53, J. Virol. 74 (20) (2000) 9441–9450.
[44] C. Berthet, et al., How adeno-associated virus Rep78 protein arrests cells completely in S phase, Proc. Natl. Acad. Sci. 102 (38) (2005) 13634–13639.
[45] R.P. Chen, A.S. Gaynor, W. Chen, Synthetic biology approaches for targeted protein degradation, Biotechnol. Adv. 37 (8) (2019) 107446.
[46] Y. Wang, Q. Fu, S.Y. Park, Y.S. Lee, S.Y. Park, D.Y. Lee, S. Yoon, Decoding cellular mechanism of recombinant adeno-associated virus (rAAV) and engineering host-cell factories toward intensified viral vector manufacturing, Biotechnol. Adv. (2024) 108322.
[47] Q. Fu, Y. Wang, J. Qin, D. Xie, D. McNally, S. Yoon, Enhanced ER protein processing gene expression increases rAAV yield and full capsid ratio in HEK293 cells, Appl. Microbiol. Biotechnol. 108 (1) (2024) 459.